Consequences of Soret–Dufour Effects, Thermal Radiation, and Binary Chemical Reaction on Darcy Forchheimer Flow of Nanofluids

Ghulam Rasool [1] , **Anum Shafiq** [2] **and Dumitru Baleanu** [3,4,5],*

[1] School of Mathematical Sciences, Zhejiang University, Hangzhou 310027, China; grasool@zju.edu.cn
[2] School of Mathematics and Statistics, Nanjing University of Information Science and Technology, Nanjing 210044, China; anum_shafiq@nuist.edu.cn
[3] Department of Mathematics, Cankaya University, Ankara 06530, Turkey
[4] Institute of Space Sciences, 077125 Magurele, Romania
[5] Department of Medical Research, China Medical University Hospital, China Medical University, Taichung 40250, Taiwan
*   Correspondence: Baleanu@mail.cmuh.org.tw

check for updates

Abstract: This research article aims to investigate the consequences of binary chemical reaction, thermal radiation, and Soret–Dufour effects on a steady incompressible Darcy–Forchheimer flow of nanofluids. Stretching surface is assumed to drive the fluid along positive horizontal direction. Brownian motion, and the Thermophoresis are accounted in particular. The governing highly nonlinear system of problems which are advanced version of Navier–Stokes equations are transformed into ordinary differential equations (ODEs) using appropriately adjusted transformations invoking symmetric property of the independent variables. The numerical approach using RK45 in connection with shooting technique is adopted to solve the final equations. Graphical approach is used to interpret the results and the values of important physical quantities are given in tabular data form. Velocity field, temperature distribution and concentration distribution are graphically analyzed for variation in respective fluid parameters. Furthermore, density graphs and stream lines are sketched for the present model. The outputs indicate a rise of temperature field in connection with thermal radiation parameter. A clear decline is noticed in velocity field for elevated values of Forchheimer number and porosity factor. The Dufour effect anticipates a rising factor for temperature distribution and the same is noticed for concentration distribution in lieu of Soret effect. Thermal radiation and binary chemical reaction has strong impact on heat transport mechanism. The results for physical quantities such as skin friction, heat and mass flux rates are given in tabular data form in last section of this study.

Keywords: Soret and Dufour effect; Darcy–Forchheimer model; stretching sheet; nanofluid; binary chemical reaction

1. Introduction

Coined by Choi [1], the advent of nanofluids drastically improved the heat transport efficiency of various fluids especially water and glycol. The formulation is purely based on the dispersion of nanometric materials such as metals, polymers, non-metals, etc. in the given base fluid such as water and other typical fluids. For efficient and improved thermal management situation that arose on the extensive and quick displacement of heat in various machinery, state of the art devices, etc. The need

for nanofluids is typically based on the logic that classic fluids have deficient performing capacity due to low thermophysical properties whereas, the technological development has greatly advanced the machinery and other equipment. Such equipment and machinery become heated while working with the typical base fluids; however, the invention of nanofluids especially those manufactured with most suited metallic ingredients have drastically controlled the heating situation of machinery. The suspension of nanoparticles that are highly capable of thermal conductivity are responsible for the enhancement in thermo-physical properties of the base fluid. The volume to surface ratio of these nanoparticles is core factor in this improvement. Some relevant studied are discussed here. For example, in the last two years numerous articles are reported targeting the enhanced heat transport mechanism on the basis of nanofluids. Aslfattahi et al. [2] reported some interesting findings in the Mxene-based emerging category of silicone oil type nanofluids, from the prospect of photo-voltaic collector, where they used Transient Hot Bridge 500 to measure the thermal conductivity of the silicone oil type Mxene nanofluid. For viscosity measurement they used Rheometer at different temperatures such as 25:25:125 degrees centigrade. Abbas et al. [3] reported an article to analyze the potential evaluation in the automotive radiators. In this study, they have confirmed the assistance of nanofluids offered to automotive radiators for enhancement in thermal management accepting the challenge of sustainability issue. Bakthavatchalam et al. [4] presented a review article on nanofluids and ionanofluids to see the comparative analysis of heat transfer improvements. A detailed comparative chart is given in this study supporting the enhancement and improvement in thermophysical attributes of the base fluids. Ghahremanian et al. [5] reported an investigation to analyze the nanofluid flow via nano-channel to see the consequences and impact of nanoparticles on condensation. They used Green-Kubo formula in their study to calculate the results. In another study, Cacua et al. [6] reported some interesting findings on stability issues of nanofluids in thermosyphon performance. The results were supported by Two-Phase-Closed mechanism. More interesting articles can be seen in [7–29] and cross references.

Flow through Darcy-medium has wide spread applications and significant worth in pharmaceutical, concoction, and modern ecological frameworks. Procedures such as geothermal exchange formats in the context of thermal management, oil supplication in various procedures, waster transfer procedures in atomic heads, water purification and water developments and numerous others. Classic Darcy model was composed of non-Darcian permeable medium which was limited version of this medium when it comes to the above mentioned applications and procedures. It was totally a restricted version for lower porosity and velocity field. For higher velocities Forchheimer updated this model accounting the squared velocity term in momentum equations. A detailed description of this model is given in Darcy [30] and Forchheimer [31]. Later on, Muskat [32] termed this medium as Darcy–Forchheimer medium (the porous medium). Relatively some works have been regarded very promising in the context of Darcy medium. For instance, Muhammad et al. [33] analyzed Darcy–Forchheimer model-based nanofluid flow bounded by an exponentially stretching flat surface in curved shape. They incorporated Cattaneo–Christov double diffusion model in their study to the enhancement in heat and mass transport via relaxation time parameters. Ambreen et al. [34] reported analytic study on hydro-thermal characteristics of nanofluid using Darcy–Forchheimer medium together with Brinkman model. The coupled multiphase Eulerian model resulted in enhancement of performance subject to low porosity factor. Ullah et al. [35] disclosed the features of Arrhenius energy in nanofluid flow under the umbrella of Darcy–Forchheimer model-based three-dimensional rotating flow subject to radiative heat transfer. They adopted NDSolve procedure for the final solutions. Huda et al. [36] produced the results for implementation of Cattaneo-Christov model in ethylene glycol-based nanofluid flow subject to Darcy–Forchheimer medium. Carbon nanotubes were considered in this theoretical study of nanofluid flow. Furthermore, Sajid et al. [37] analyzed

the convenience of a Darcy–Forchheimer flow modeled by Maxwell using nonlinear type of thermal radiation via stretching surface.

The combined study of heat and mass flux phenomena involves the flow driven by the difference of densities caused by the gradients of temperature and concentration distributions at the same time together with material composition. Soret relates with the mass flux phenomena caused by the thermal diffusion, while heat flux (energy flux) developed by the solute difference is typically known as the Dufour effect. The mixtures between gases with lighter and medium molecular weights are dealt with by the Soret effect. There are many practical applications linked with this phenomena, such as chemical and geophysical engineering. Researchers showed immense interest in these two aspects and they were as a result involved in various studies. For instance, Jiang et al. [38] reported interesting results in simultaneously heat and mass transport mechanisms via species inter-diffusion process under the direct influence of Dufour and Soret effect. Natural convection was examined via evaporation and condensation phenomena. Liu et al. [39] incorporated multiple-relaxation phenomena via lattice Boltzmann theory to implement the dual-diffusive natural convective flow. Dufour and Soret impacts are involved. They revealed that double-diffusive natural convection can be done easily under the direct influence of Soret and Dufour effects. Sardar et al. [40] analyzed mixed convection phenomena in Carreau nanofluid flow bounded by wedge with the effects of Soret and Dufour. The outcomes indicated that there is a considerable decrease in heat flux for enhanced values of Brownian diffusion parameter.

A typical chemical reaction is always dependent on a decent quantity of activation energy no matter it is linear or binary, to start off. The Arrhenius equations is therefore, necessary for a model involving chemical reaction to calculate the amount of this activation energy. This equations describes the variation of temperature within the system due to the chemical reaction phenomena. Several industrial applications are linked with fluid flow analysis based on chemical reaction due to which researchers have adopted this factor frequently in their models. For instance, Hamid et al. [41] reported some good results on the impact of such chemical reaction using the equation of activation energy in the MHD Williamson nanofluid flow. The heat flux de-escalates for larger chemical reaction parameter. Dhlamini et al. [42] analyzed the impact of activation energy as well as the binary chemical reaction on mixed convection yielded by the use of convective boundary. The Biot number increases the concentration distribution of chemical species. Khan et al. [43] reported dual solutions for the impact of activation energy on the flow MHD titanium alloy (Ti_6Al_4V)-based nanofluid with a cross flow structure. A chemical reaction (binary) term and thermal radiation was involved in this study. Important results have been reported by Dulal Pal et al. [44] regarding the impact of chemical reaction and Surot and Dufour factors in fluid flow analysis.

Numerous research articles are reported in the context of nanofluids flow bounded by stretching surfaces under the umbrella of Buongiorno's model. Different methodologies were adopted to tackle the heat and transport problems as reported in the literature mentioned above. However, there are still gap in the studies on nanofluids in many aspects. Here in this study, we incorporated the Darcy–Forchheimer relation together with Soret–Dufour effects and binary chemical reaction subject to linear stretching with uniform impact of MHD to fill the gap in research mentioned in preceding section. Thermal radiation is another important factor involved in this study. Furthermore, Brownian motion, and thermophoresis are considered in particular. The modeled problem is solved numerically using numerical RK45-Scheme with the help of Shooting technique. Up to the understanding and knowledge of authors, this formulation has not been reported in the literature. The results are highly recommended for industrial and engineering applications of nanofluids as well as in chemical engineering. The paper is organized as follows: Modeling of the problem with a literature review of the topic is followed

by the numerical solution of the problem. The detailed discussion followed by a comparison with previously published literature is concluded with salient findings noted in last section.

2. Mathematical Modeling

We consider a steady incompressible Darcy–Forchheimer model-based nanofluid flow maintained over a linearly stretching sheet under the umbrella of Buongiorno's model to tackle the Brownian motion and thermophoresis phenomena. The major contribution comes from Soret–Dufour effects and binary chemical reaction which are the novel factors in this study. The linear stretching property of the sheet with thermal radiation impact are the driving factors for the fluid. The two dimensions are taken in Cartesian coordinates with x-axis alongside the flow and y-axis normal the surface of flow. The fluid flow is taken along positive x-direction while the velocity along surface normal to the x-direction is assumed to be zero. Typical velocity components are assumed as u, v for horizontal and vertical directions, respectively. The governing problems (see for example [21,34,41,44,45]) are given below,

$$\frac{\partial u}{\partial x} + \frac{\partial v}{\partial y} = 0, \tag{1}$$

$$u\frac{\partial u}{\partial x} + v\frac{\partial u}{\partial y} = \nu\frac{\partial^2 u}{\partial y^2} - \left(\frac{\nu}{K} + Fu\right)u - \frac{\sigma B_0^2}{\rho_f}u, \tag{2}$$

$$u\frac{\partial T}{\partial x} + v\frac{\partial T}{\partial y} = \alpha\frac{\partial^2 T}{\partial y^2} - \frac{1}{\rho c_f}\frac{\partial q_r}{\partial y} + \frac{(D_T k_t)}{C_s C_p}\frac{\partial^2 C}{\partial y^2} + \frac{\sigma B_0^2}{\rho c_f}u^2 + \frac{\mu}{K\rho c_f}u^2 + \tau\left(D_B\left(\frac{\partial C}{\partial y}\frac{\partial T}{\partial y}\right) + \frac{D_T}{T_\infty}\left(\frac{\partial T}{\partial y}\right)^2\right), \tag{3}$$

$$u\frac{\partial C}{\partial x} + v\frac{\partial C}{\partial y} = D_B\left(\frac{\partial^2 C}{\partial y^2}\right) + \frac{D_T k_t}{T_\infty}\frac{\partial^2 T}{\partial y^2} - K\left(\frac{T}{T_\infty}\right)^n \exp\left(\frac{-E_1}{KT}\right)(C - C_\infty), \tag{4}$$

subject to

$$u = u_w = zx, \quad v = 0, \quad (T, C) = (T_w, C_w) \quad \text{at} \quad y = 0, \tag{5}$$

$$u = 0, \quad (T, C) = (T_\infty, C_\infty) \quad \text{as} \quad y \to \infty. \tag{6}$$

Define,

$$\phi(\eta) = \frac{C - C_\infty}{C_w - C_\infty}, \quad \theta(\eta) = \frac{T - T_\infty}{T_w - T_\infty}, \quad \eta = y\sqrt{\frac{z}{\nu}}, \tag{7}$$
$$u = zx\frac{\partial f}{\partial \eta}, \quad v = -\sqrt{z\nu}f(\eta),$$

Using (7) in (1)–(6), we have

$$f''' - f'^2 + ff'' - M_1^2 f' - F_r\left(f'\right)^2 - \lambda f' = 0, \tag{8}$$

$$\left(1 + \frac{4}{3}R_1\right)\theta'' + \theta'^2 + Prf\theta' + D_f Pr\phi'' + PrEc(M_1^2)f'^2 + EcPr\lambda f'^2 + \left(N_t\theta'^2 + N_b\theta'\phi'\right) = 0, \tag{9}$$

$$\phi'' + Scf\phi' + S_r\theta'' - ScK_1 N_b(1 + \delta_1\theta)^{n_1}\exp\left(\frac{-E_1}{1 + \delta_1\theta}\right)\phi = 0, \tag{10}$$

$$f = 0, \quad \theta = \phi = f' = 1, \quad \text{at} \quad \eta = 0$$
$$\theta = f' = \phi = 0 \quad \text{as} \quad \eta \to \infty. \tag{11}$$

Here, M_1 is magnetic number such that $M_1^2 = \frac{\sigma B_0^2}{z\rho_f}$, $\lambda = \frac{\nu}{Kz}$ is porosity, $\frac{C_b}{\sqrt{K}} = F_r = Fx$ is Forchheimer number, $Pr = \frac{\nu}{\alpha}$ is Prandtl number, $Nb = \frac{(C_w - C_\infty)\tau D_B}{\nu}$ is Brownian motion factor, $Nt = \frac{(T_w - T_\infty)\tau D_T}{\nu T_\infty}$ is Thermophoretic force factor and $Sc = \frac{\nu}{D_B}$ is Schmidt number, $R_1 = \frac{4\sigma T_\infty^3}{kk_1}$ is the radiation

derived from q_r using the Taylors expansion by neglecting higher order terms. $D_f = \frac{D_T k_t (C_w - C_\infty)}{\nu C_s C_p (T_w - T_\infty)}$ is the Dufour number while $S_r = \frac{D_T k_t (T_w - T_\infty)}{\nu T_\infty (C_w - C_\infty)}$ is Soret number. $E_1 = \frac{E}{kT_\infty}$ is used for activation energy with $K_1 = (C_w - C_\infty)$ as the chemical reaction parameter.

3. Methodology

The numerical approach using RK45 in connection with shooting technique is adopted to solve the final governing system of Ordinary differential equations. Scheme is given as follows:

$$f = f, \tag{12a}$$

$$f' = m, \tag{12b}$$

$$f'' = m' = n, \tag{12c}$$

$$f''' = m'' = n' = m^2 - fn + M_1^2 m + \lambda m + F_r m^2, \tag{12d}$$

$$\theta = \theta, \tag{12e}$$

$$\theta' = p, \tag{12f}$$

$$\theta'' = p', \tag{12g}$$

$$\phi = \phi, \tag{12h}$$

$$\phi' = q, \tag{12i}$$

$$\phi'' = q', \tag{12j}$$

$$\left(1 + \frac{4}{3} R_1\right) \theta'' = \left(1 + \frac{4}{3} R_1\right) p' = -p^2 - Pr f p - D_f Pr q' - Pr Ec M_1^2 m^2 - \left(N_t p^2 + N_b pq\right), \tag{12k}$$

$$\phi'' = m' = -Sc f q - S_r p' + Sc K_1 N_b \left(1 + \delta_1 \theta\right)^{n_1} \exp\left(\frac{-E_1}{1 + \delta_1 \theta}\right) \phi, \tag{12l}$$

Subject to

$$f = 0, \quad \theta = \phi = m = 1, \qquad \text{at} \qquad \eta = 0, \tag{13a}$$

$$\theta = \phi = m = 0, \qquad \text{as} \qquad \eta \to \infty. \tag{13b}$$

Results are plotted in graphs.

4. Results and Discussion

We consider a viscous incompressible nanofluid fluid flow under the umbrella of Darcy–Forchheimer model using a linearly stretchable sheet. The major contribution comes from Soret–Dufour effects and binary chemical reaction which are the novel factors in this study. The linear stretching property of the sheet with thermal radiation impact, Thermophoresis and Brownian diffusion all together are the driving factors for the fluid. From Figures 1–3 we notice the impact of Porosity factor, magnetic parameter and Forchheimer (inertia factor) number on the fluid momentum. Velocity profile receives much reduction for elevated values of these three parameters within the domain of suitable convergent values for the given parameters. Clearly the rising effect of porosity and inertial boost up the friction offered to the fluid flow and thereafter, the result is opposite. In case of magnetic parameter, the sudden bumps in the way of fluid motion offered by the in-field magnetic impact are causing disturbance for smooth movement of the fluid. Thus, the profile receives much reduction in all the three cases. In Figures 4 and 5 the impact of Brownian diffusion and Thermophoresis is analyzed for their elevated values versus the thermal distribution of the fluid flow analysis. In both cases, a rise in thermal state is noticed. The in-predictive motion appearing within the nanoparticles due to the Brownian diffusion speeds up with stronger thermophoretic force. In addition, consequent

results is the enhancement of thermal state of the fluid. The radiation parameter is also an important factor in this study and relevant information about the behavior of thermal profile for variation in radiation parameter is given in Figure 6. One can see a prominent rising trend in thermal state of the fluid due to larger values of radiation factor especially when radiation impact approaches 1 (infinity). This trend is justified because the radiation parameter provides convenient and easier convection ground to the thermal distribution. The thermal state receives enhancement for larger values of Dufour number due to the heat generated by the temporary concentration gradient which is the constituent element of Dufour effect shown in Figure 7. Figures 8 and 9 are the influential displays of variation noted in concentration of the nanoparticles for elevated values of Brownian diffusion parameter and thermophoresis. An equally opposite trend is noticed in this case. The rising concentration distribution represents the variation against Brownian diffusion whereas, the reduction is linked to the thermophoresis. The consequent results of Schmidt number on concentration distribution is given in Figure 10. The inverse proportion of kinematic viscosity with Brownian diffusion results a rise in concentration distribution. Concentration distribution receives prominent rise for augmented values of Soret factor given in Figure 11. The impact of Binary chemical reaction is given in Figure 12. A reduction near the surface is noticed in higher values of chemical reaction parameter. The non-dimensional number δ_1 impacts on the concentration profile as a declining factor as shown in Figure 13. Three dimensional display of variation in Nusselt number is given in Figures 14 and 15 for Brownian diffusion and Dufour number, respectively. Figures 16 and 17 are the sketch of stream density at fixed values of porosity factor and magnetic impact parameter. A slight variation is noticed which disappears towards infinity. Table 1 gives a validation of present results for velocity field with previously published literature which is found in agreement. The numerical results of skin-friction and Nusselt number are given in Tables 2 and 3, respectively. As per the data given in Tables 2 and 3, the numerical values of skin-friction are positively affected by the three parameters involved in momentum equations. Dufour number enhances the Nusselt number while a reduction in Sherwood number is noticed for the same parameter. A similar trend is appeared in case of Soret number. For chemical reaction, the heat flux reduces while the mass flux enhances.
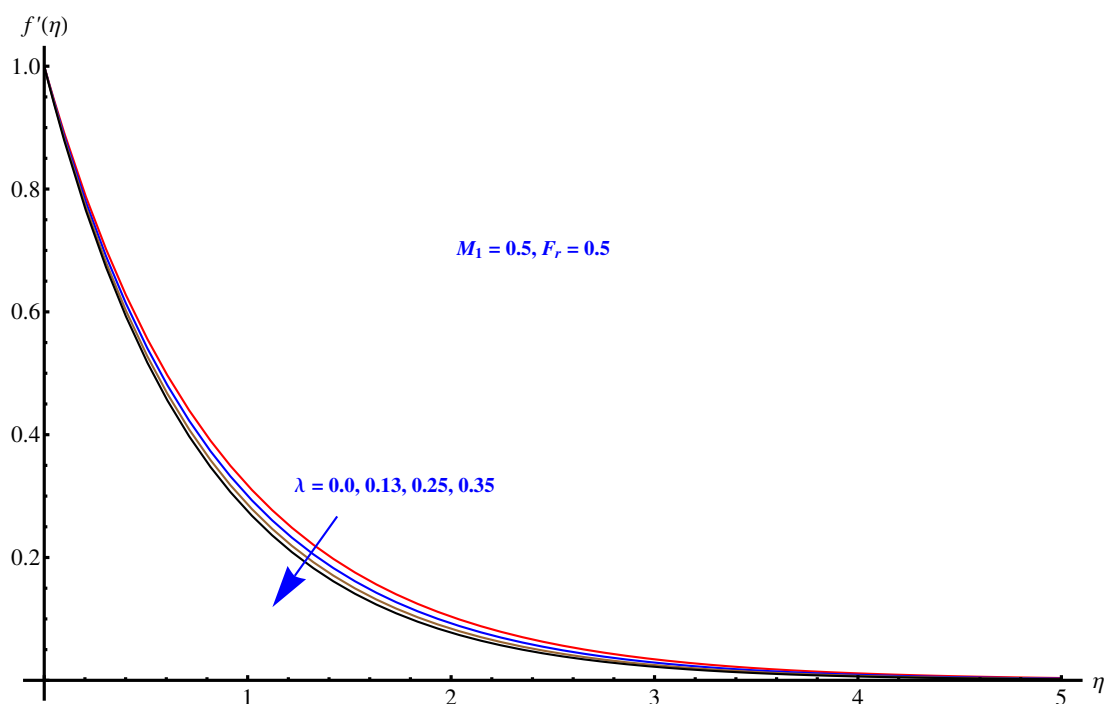

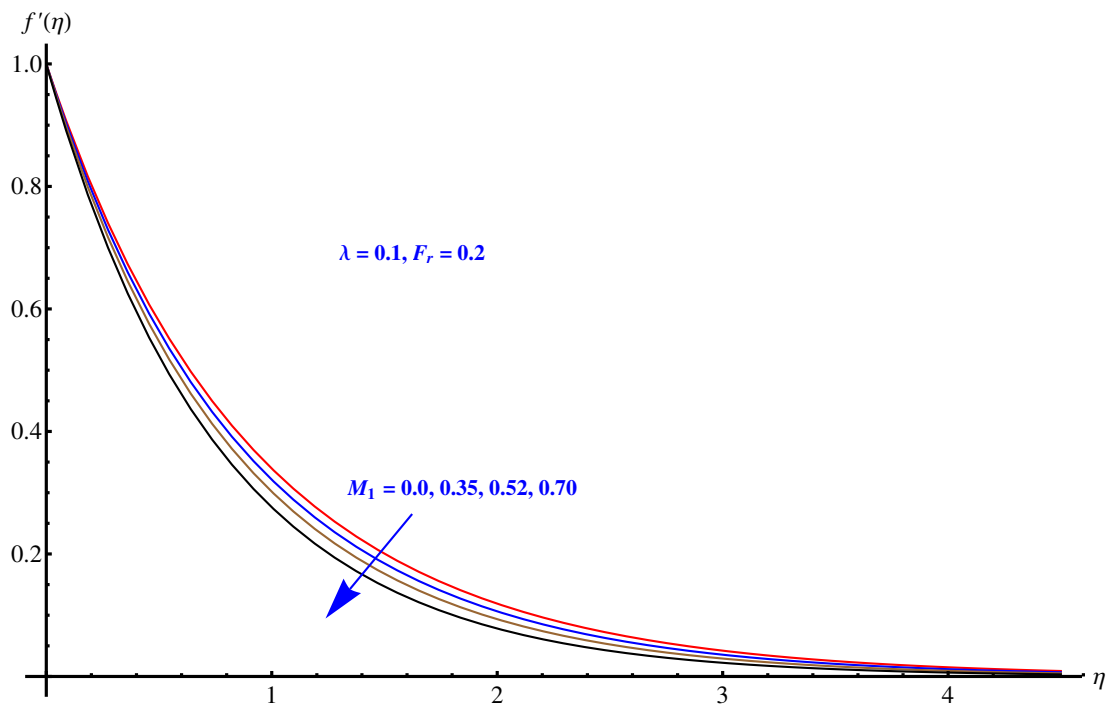**Figure 1.** Impact of porosity factor λ on $f'(\eta)$.

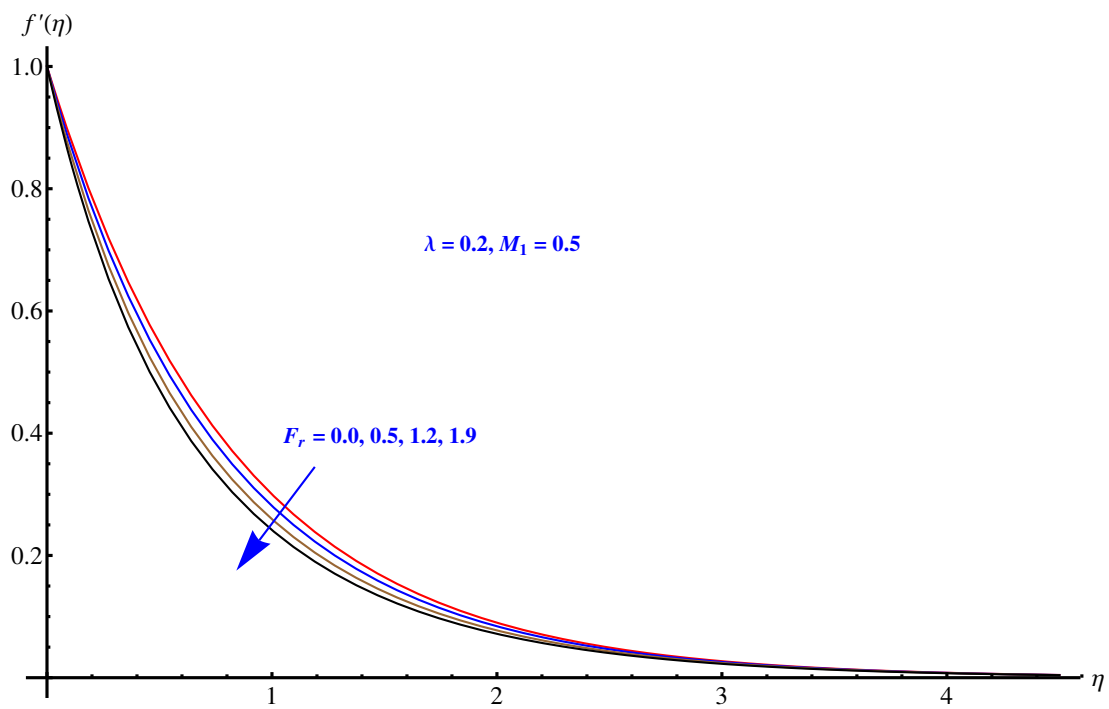**Figure 2.** Impact of magnetic parameter M_1 on $f'(\eta)$.

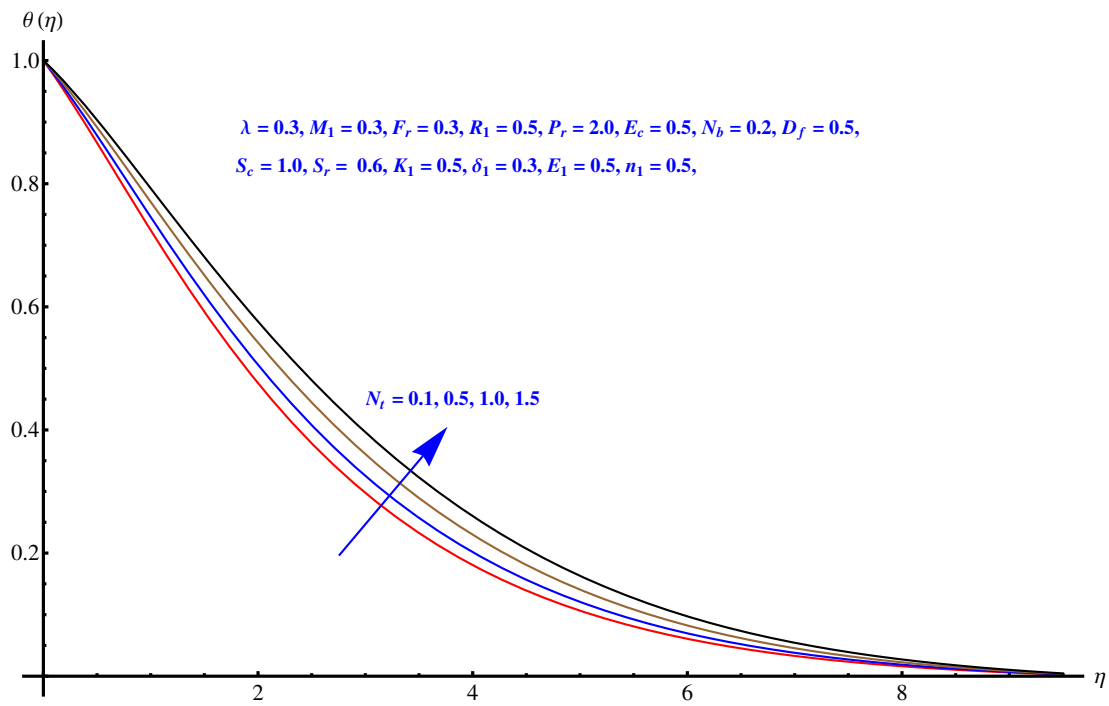**Figure 3.** Impact of Forchheimer number F_r on $f'(\eta)$.

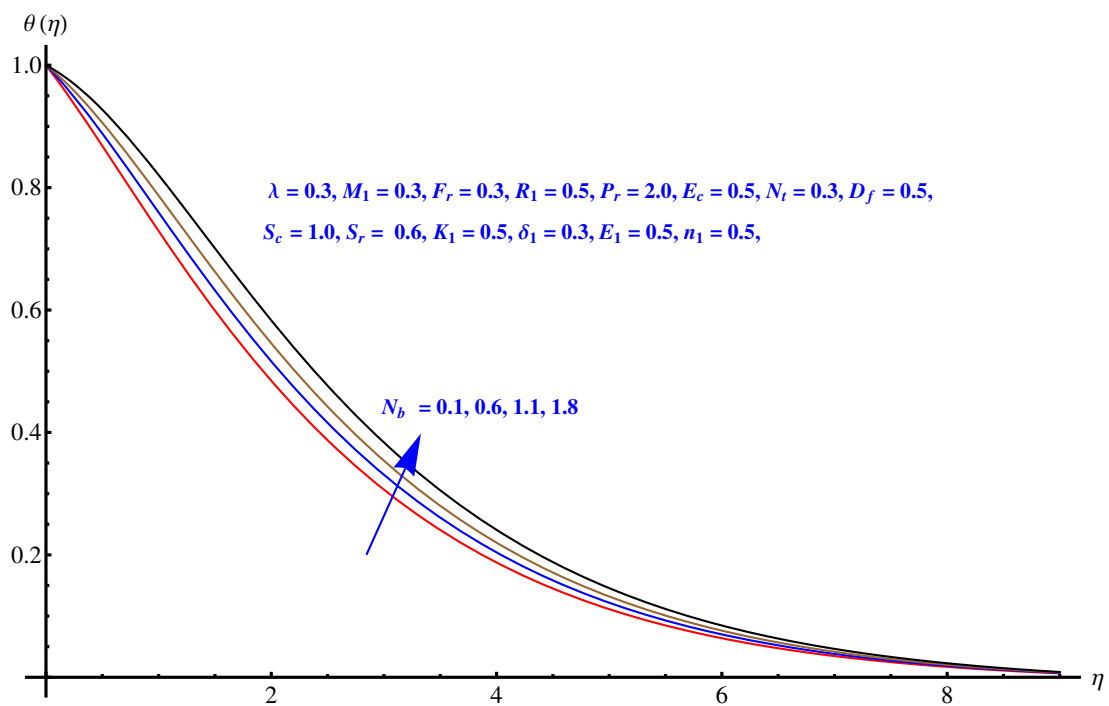**Figure 4.** Impact of thermophoresis N_t on $\theta(\eta)$.

Figure 5. Impact of Brownian motion parameter N_b on $\theta(\eta)$.
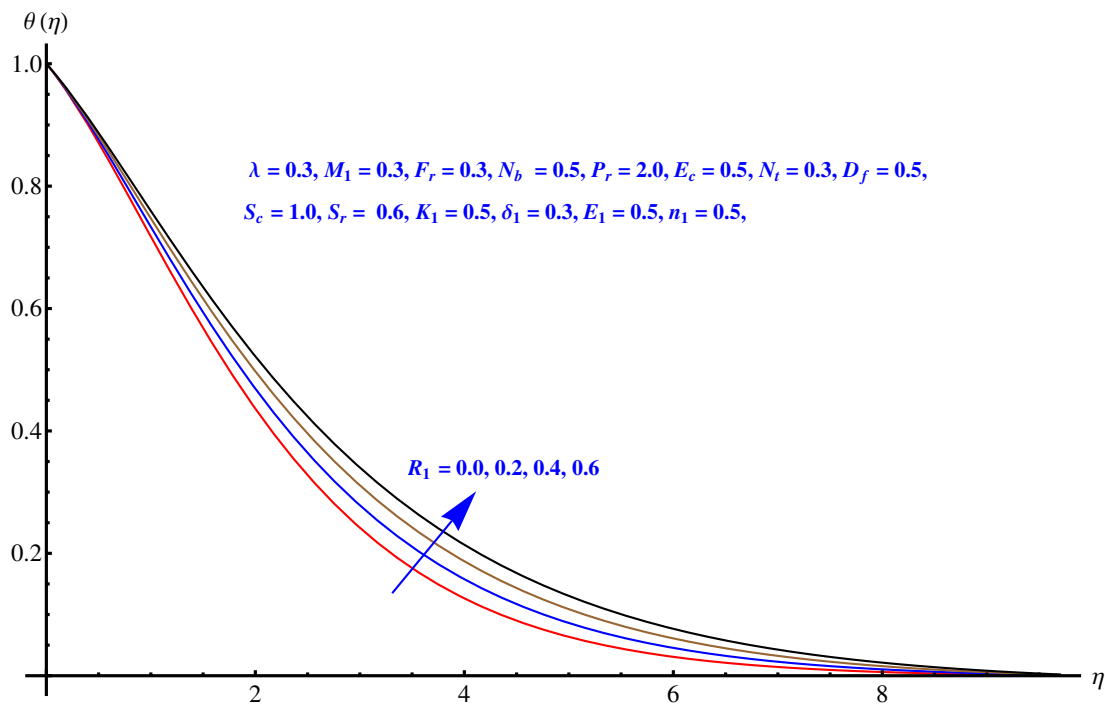
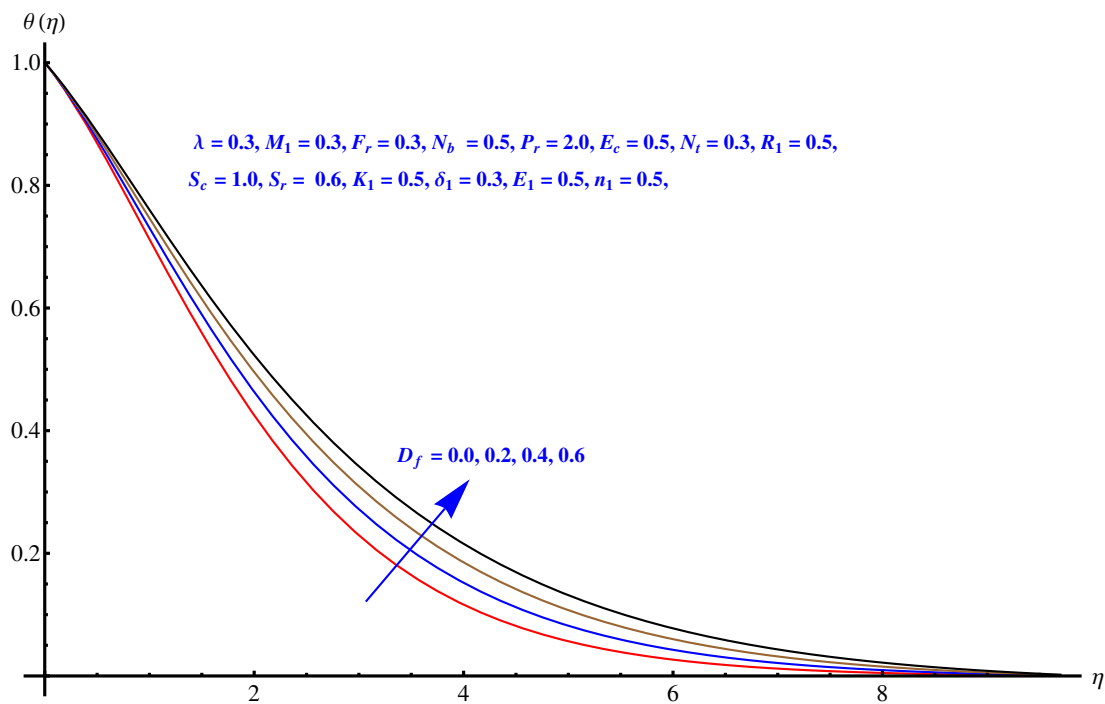**Figure 6.** Impact of thermal radiation parameter R_1 on $\theta(\eta)$.

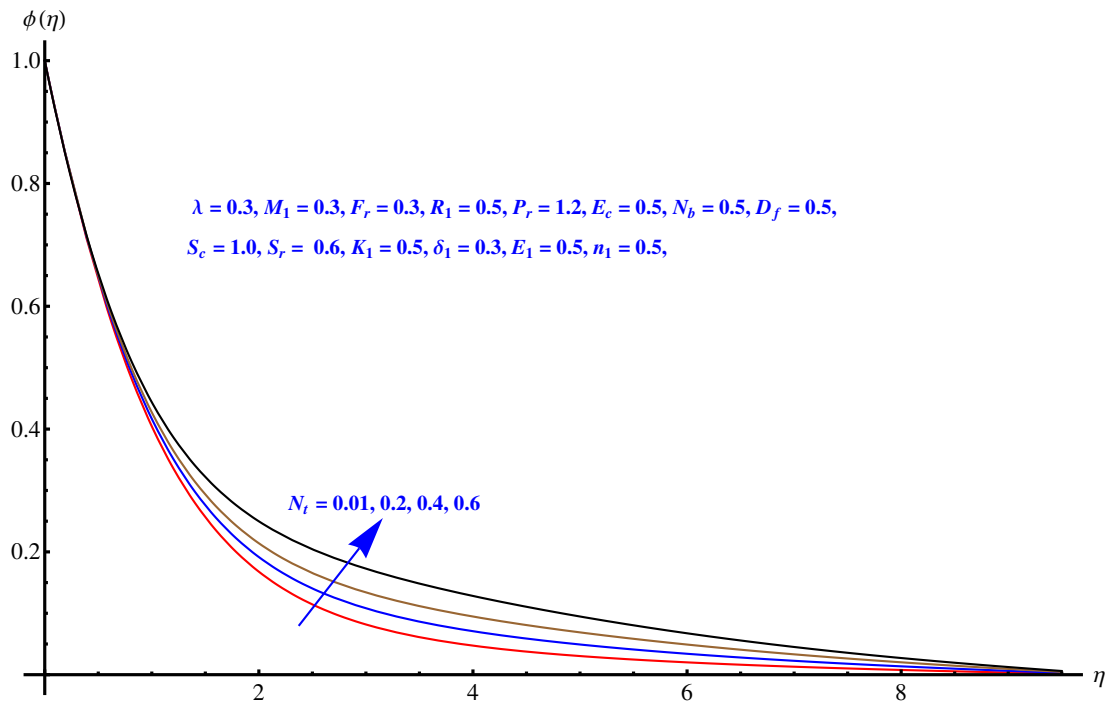**Figure 7.** Impact of Dufour parameter D_f on $\theta(\eta)$.

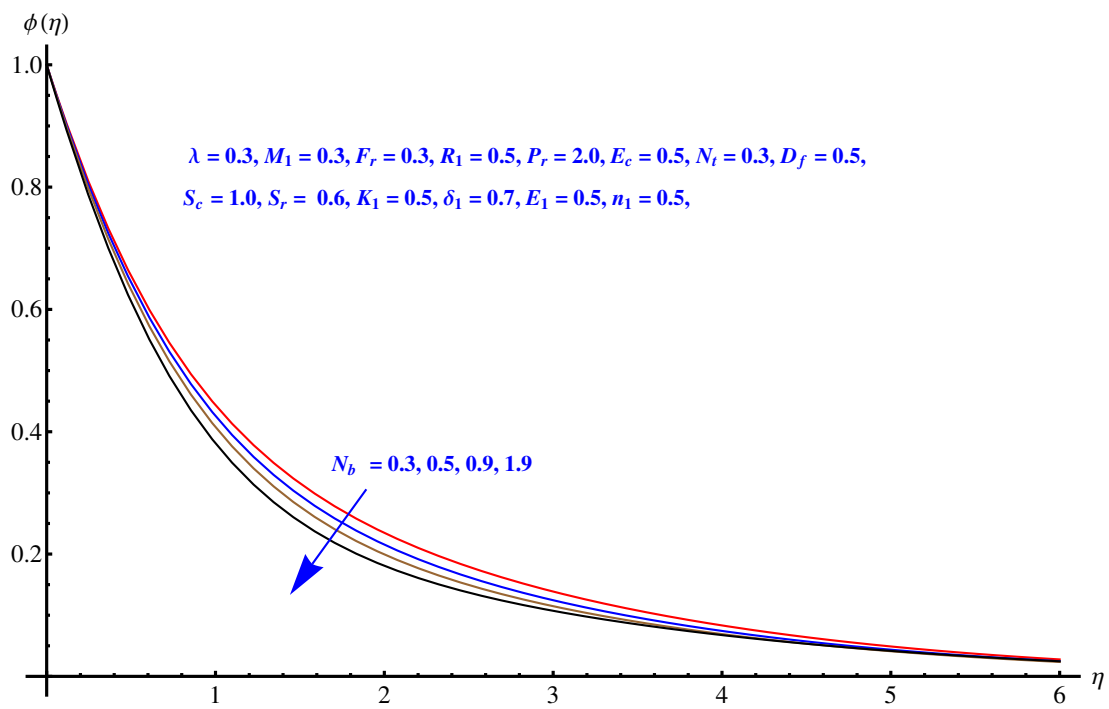**Figure 8.** Impact of thermophoresis N_t on $\phi(\eta)$.

Figure 9. Impact of Brownian motion parameter N_b on $\phi(\eta)$.
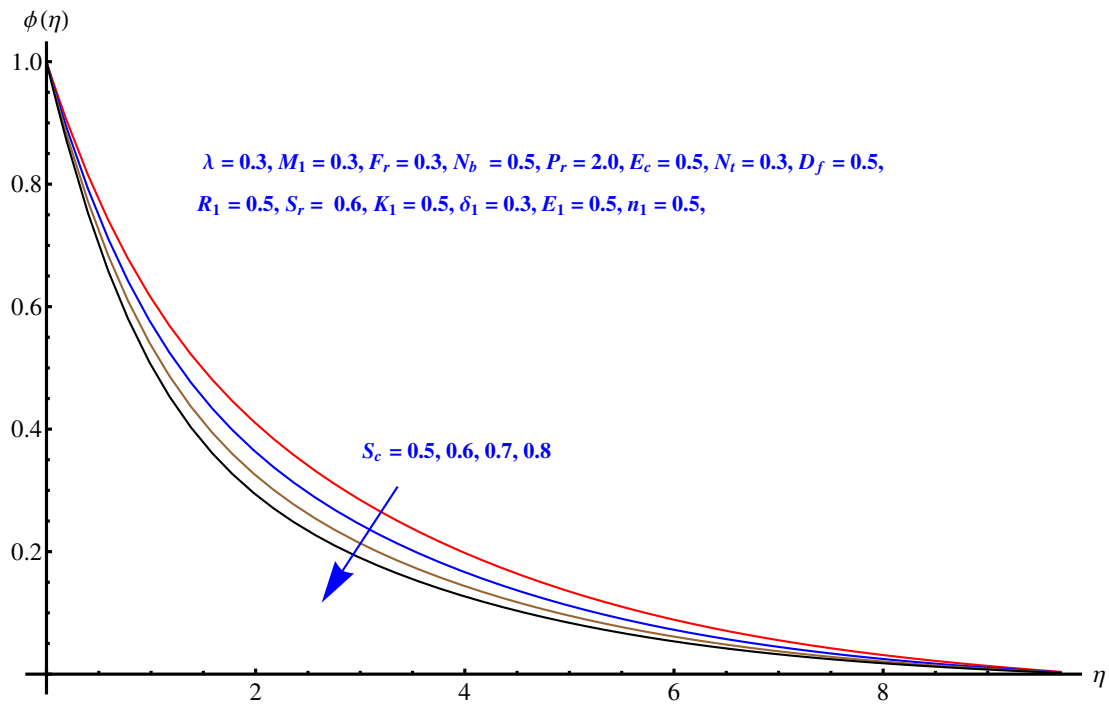
Figure 10. Impact of Schmidt number Sc on $\phi(\eta)$.

$\lambda = 0.3, M_1 = 0.3, F_r = 0.3, N_b = 0.5, P_r = 2.0, E_c = 0.5, N_t = 0.3, D_f = 0.5,$
$R_1 = 0.5, S_r = 0.6, K_1 = 0.5, \delta_1 = 0.3, E_1 = 0.5, n_1 = 0.5,$

$Sc = 0.5, 0.6, 0.7, 0.8$
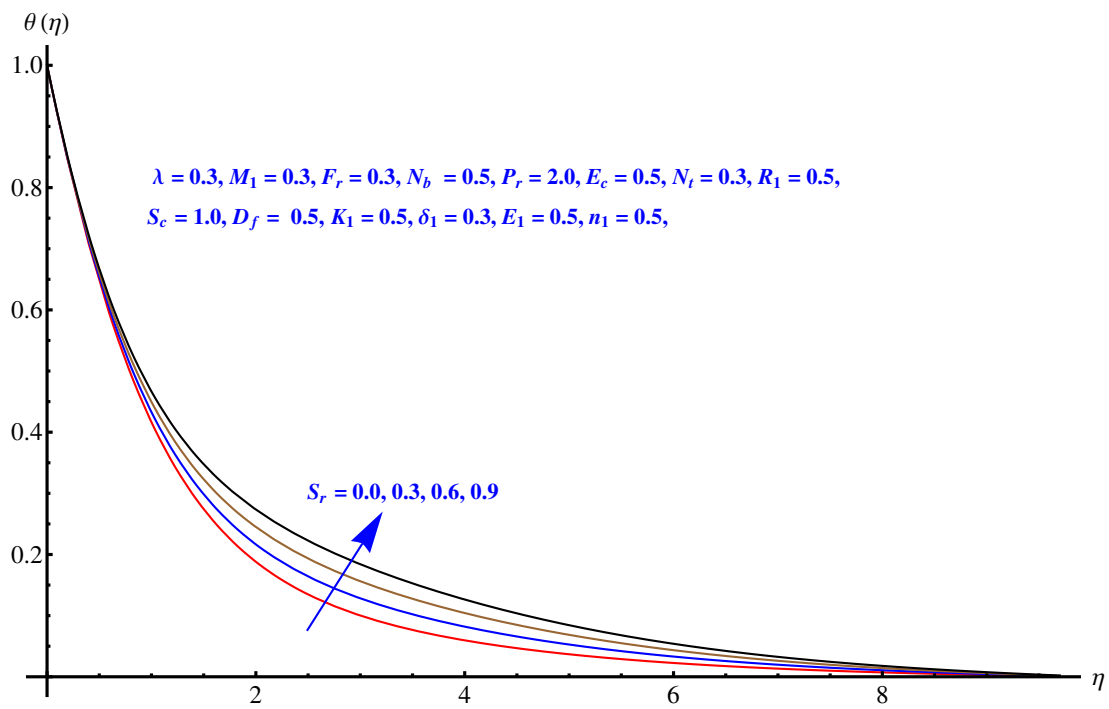
Figure 11. Impact of Soret parameter Sr on $\phi(\eta)$.

$\lambda = 0.3, M_1 = 0.3, F_r = 0.3, N_b = 0.5, P_r = 2.0, E_c = 0.5, N_t = 0.3, R_1 = 0.5,$
$Sc = 1.0, D_f = 0.5, K_1 = 0.5, \delta_1 = 0.3, E_1 = 0.5, n_1 = 0.5,$

$S_r = 0.0, 0.3, 0.6, 0.9$

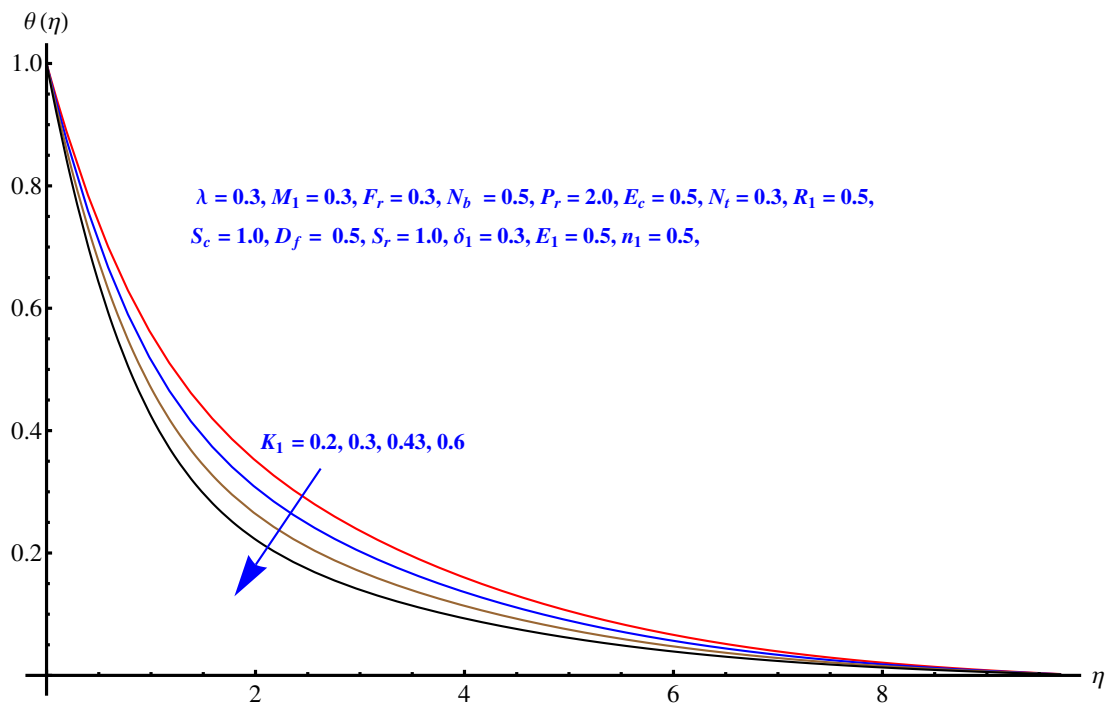**Figure 12.** Impact of chemical reaction parameter K_1 on $\phi(\eta)$.
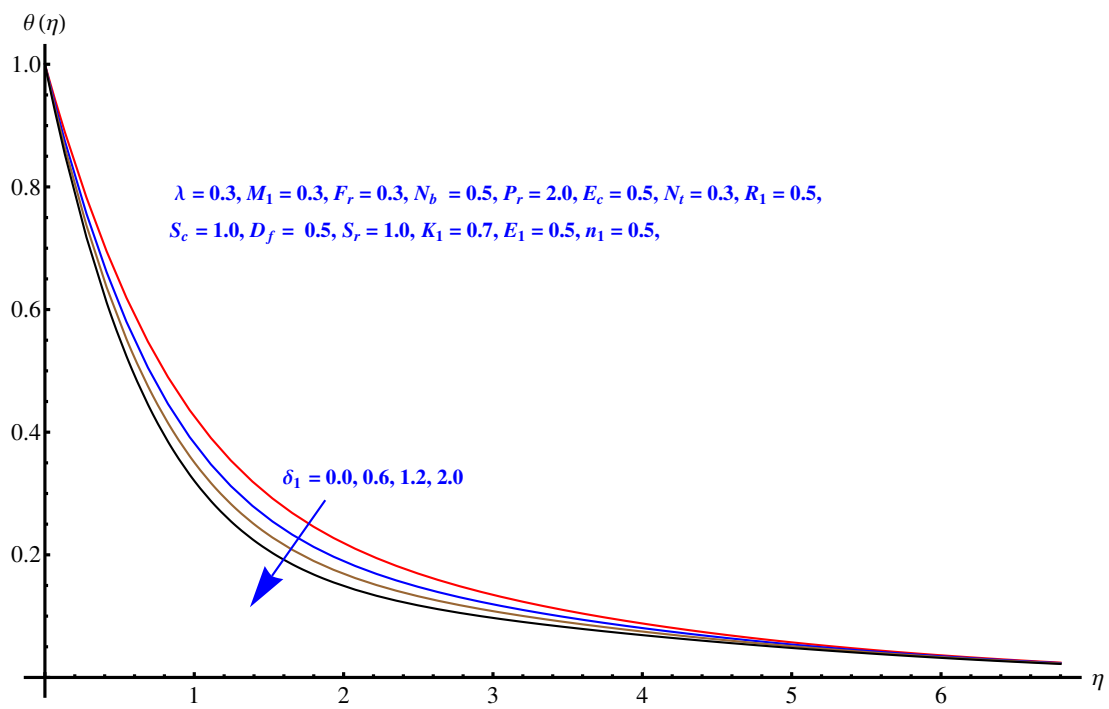
Figure 13. Impact of dimensionless parameter δ_1 on $\phi(\eta)$.
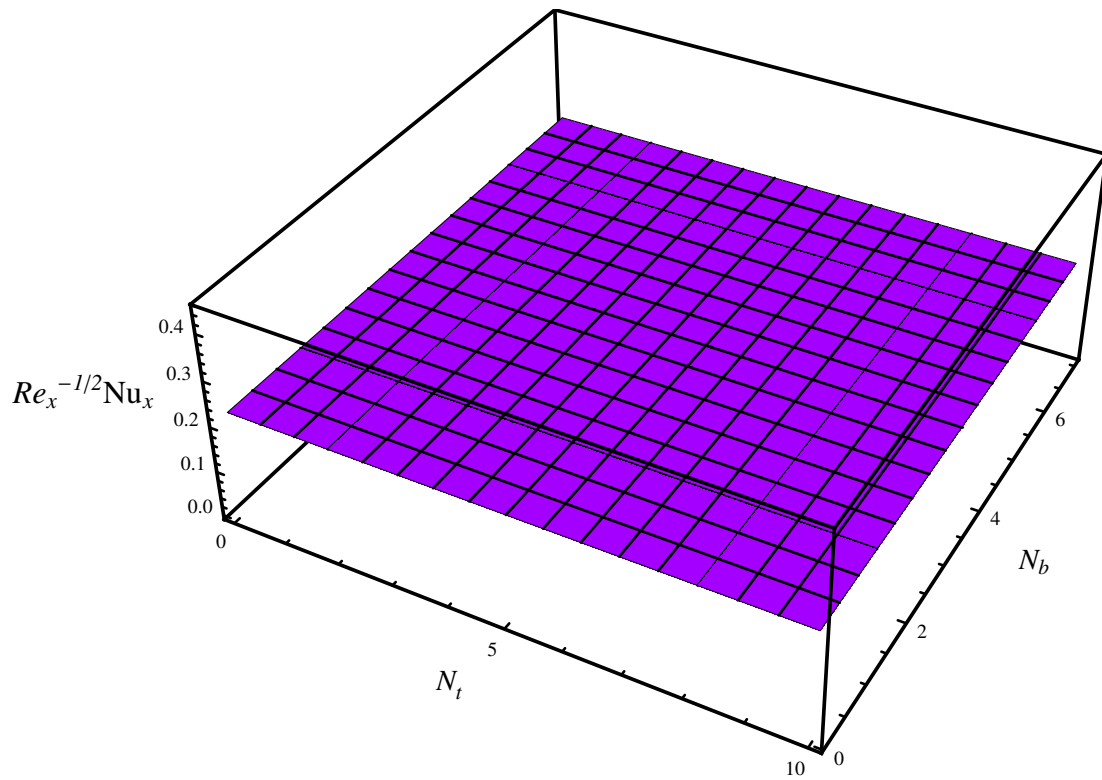
Figure 14. Impact of Brownian motion and thermophoresis parameter (N_b and N_t) on Nusselt number (3D analysis).
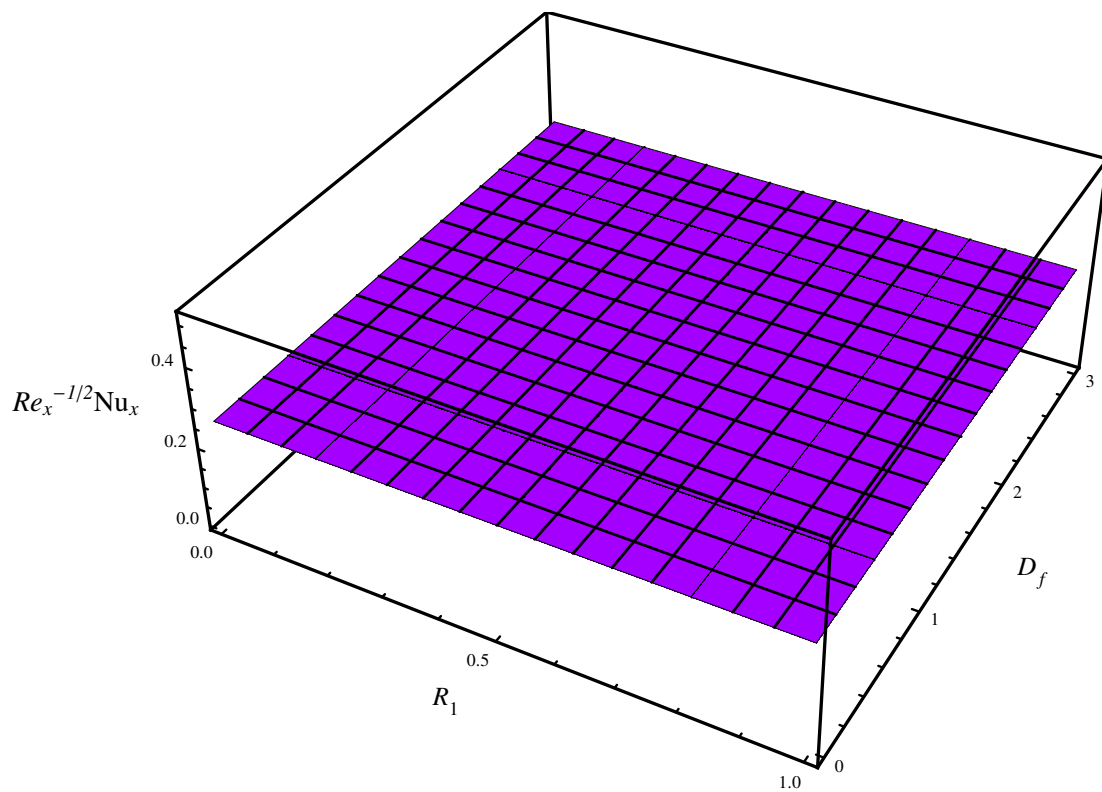
Figure 15. Impact of thermal radiation parameter and Dufour parameter (R_- and D_-f) on Nusselt number (3D analysis).
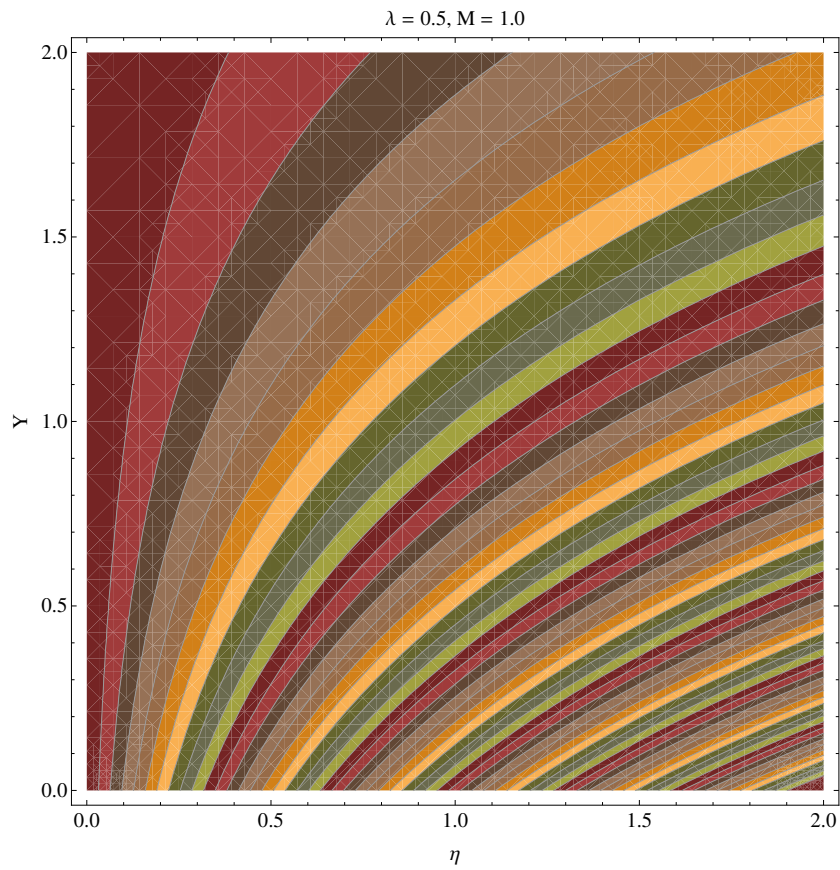
Figure 16. Stream density at $\lambda = 0.5, M_1 = 1.0$.

Figure 17. Stream density at $\lambda = 1.0, M_1 = 1.0$.

Table 1. Compararison of $-f''(0)$ with Turkyilmazoglu [45] at $F_r = 0$ and $M_1 = 0$.

λ	Turkyilmazoglu [45]	Present Results
0.0	1.00000	1.00000
0.5	1.22474	1.22475
1.0	1.41421	1.41421

Table 2. Numerical Data of skin-friction.

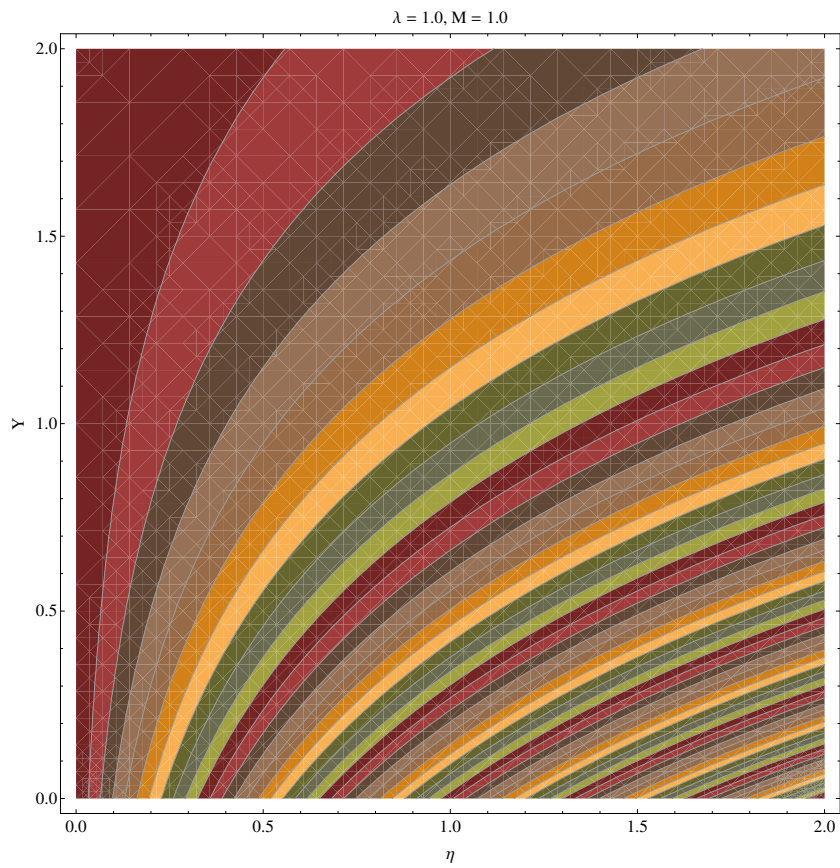| M_1	F_r	λ	$-Re_x C_x$
0.0	0.3	0.2	1.19526
0.3			1.23247
0.6			1.26013
0.3	0.0	0.6	1.17898
	0.2		1.23247
	0.4		1.28393
0.3	0.2	0.0	1.10346
		0.3	1.23247
		0.9	2.92884

Table 3. Data of Nusselt and Sherwood factors at $E_1 = 5/10, n_1 = 5/10$.

M_1	F_r	λ	R_1	Pr	N_t	N_b	Ec	D_f	S_c	S_r	K_1	δ_1	Nusselt	Sherwood
0.0	0.2	0.3	0.3	1.0	0.1	0.2	0.5	1.0	1.0	0.6	0.5	0.3	0.274811	0.815813
0.3													0.260908	0.819974
0.6													0.218650	0.819500
0.3	0.0	0.3	0.3	1.0	0.1	0.2	0.5	1.0	1.0	0.6	0.5	0.3	0.263533	0.822265
	0.2												0.260908	0.819974
	0.4												0.258430	0.817822
0.3	0.2	0.0	0.3	1.0	0.1	0.2	0.5	1.0	1.0	0.6	0.5	0.3	0.310726	0.805497
		0.3											0.260908	0.819974
		0.6											0.193255	0.766100
0.3	0.2	0.3	0.0	1.0	0.1	0.2	0.5	1.0	1.0	0.6	0.5	0.3	0.199287	0.817020
			0.3										0.260908	0.819974
			0.6										0.316413	0.822757
0.3	0.2	0.3	0.3	1.0	0.1	0.2	0.5	1.0	1.0	0.6	0.5	0.3	0.260908	0.819974
				1.5									0.309319	0.803200
				2.0									0.344432	0.789807
0.3	0.2	0.3	0.3	1.0	0.1	0.2	0.5	1.0	1.0	0.6	0.5	0.3	0.260908	0.819974
					0.3								0.250746	0.809926
					0.6								0.236296	0.808286
0.3	0.2	0.3	0.3	1.0	0.1	0.2	0.5	1.0	1.0	0.6	0.5	0.3	0.260908	0.819974
						0.4							0.243492	0.832379
						0.6							0.226979	0.839791
0.3	0.2	0.3	0.3	1.0	0.1	0.2	0.0	1.0	1.0	0.6	0.5	0.3	0.302139	0.792777
							0.5						0.260908	0.819974
							1.0						0.219501	0.847286
0.3	0.2	0.3	0.3	1.0	0.1	0.2	0.5	0.5	1.0	0.6	0.5	0.3	0.284057	0.816328
								1.0					0.260908	0.819974
								1.5					0.242852	0.823397
0.3	0.2	0.3	0.3	1.0	0.1	0.2	0.5	1.0	0.5	0.6	0.5	0.3	0.263354	0.536129
									1.0				0.260908	0.819974
									1.5				0.259807	1.043000
0.3	0.2	0.3	0.3	1.0	0.1	0.2	0.5	1.0	1.0	0.0	0.5	0.3	0.260260	0.831351
										0.3			0.260583	0.825715
										0.6			0.260908	0.819974
0.3	0.2	0.3	0.3	1.0	0.1	0.2	0.5	1.0	1.0	0.6	0.0	0.3	0.264266	0.429678
											0.3		0.261754	0.697219
											0.6		0.260593	0.87324
0.3	0.2	0.3	0.3	1.0	0.1	0.2	0.5	1.0	1.0	0.6	0.5	0.0	0.261153	0.766559
												0.3	0.260908	0.819974
												0.6	0.260705	0.865225

5. Conclusions

In this research article, we investigated the consequences of Soret–Dufour effects, thermal radiation, and binary chemical reaction on steady incompressible Darcy–Forchheimer flow of nanofluids under the umbrella of Buongiorno's model. Brownian motion and thermophoresis are accounted in particular. The salient features of this research are listed below:

- Velocity profile receives much reduction for elevated values of porosity factor and Forchheimer number due to enhancement in friction offered to the fluid flow.
- Thermal state is seen rising for elevated Brownian diffusion and thermophoresis.
- The radiation parameter is responsible for a rising trend in thermal state of the fluid for easy and convenient heat convection.
- Concentration distribution receives prominent rise for augmented values of Soret factor.
- A reduction near the surface in concentration distribution is noticed in higher values of chemical reaction parameter.
- Thermal state receives enhancement for augmented numerical values of Dufour number.
- Skin friction is augmented for all the three parameters that are used in momentum equation i.e., Magnetic impact, Forchheimer number and Porosity.
- The skin-friction is positively affected by the three parameters involved in momentum equation.
- Dufor and Soret numbers appear as a source of enhancement in Nusselt number.
- Chemical reaction results in reduction of the heat flux.

Nomenclature

RK45	Runge-Kutta 45 Method
PDE	Partial Differential Equation
MHD	Magnetohydrodynamics
ODE	Ordinary Differential Equation
x, y	Cartesian distance coordinates/m
u, v	Velocity coordinates/m$\cdot$s^{-1}
z	Stretching rate/s^{-1}
$u_w = zx$	Velocity (stretching)/m$\cdot$s^{-1}
B_0	Magnetic impact/intensity/A$\cdot$m^{-1}
μ	Dynamic viscosity/Pa$\cdot$s
ρ_f	Density/kg$\cdot$m^{-3}
ν	Kinematic viscosity/m$^2\cdot$s^{-1}
D_T	thermophoresis
D_B	Brownian diffusion
C	Concentration distributions/kg$\cdot$m^{-3}
T	Temperature distributions /K
$(\rho c)_{np}$	Nanoparticles' heat capacity/J$\cdot$m$^{-3}\cdot$k^{-1}

σ	Electric conductivity of the base fluid$/(\Omega\,\text{m})^{-1}$
C_b	Drag force coefficient
$(\rho c)_{fl}$	Fluid's heat capacity$/\text{J}\cdot\text{m}^{-3}\cdot\text{k}^{-1}$
τ	Ratio of heat capacity of fluid and nanoparticles
K	Permeability
σ'	Stephen boltzmann constant
q_r	Radiative heat flux
α	Thermal diffusivity$/\text{m}^2\cdot\text{s}^{-1}$
$k\prime$	Mean absorption constant
k	Thermal conductivity$/\text{W}\cdot\text{m}^{-1}\cdot\text{K}^{-1}$

Dimensionless Parameters

M_1	Magnetic parameter
Sc	Schmidt number
Pr	Prandtl number
N_t	thermophoresis
N_b	Brownian diffusion
Nu_x	Nusselt factor
Sh_x	Sherwood factor
λ	Porosity
F_r	Forchheimer number
Ec	Eckert number
R_1	Radiation parameter
D_f	Dufour parameter
S_r	Soret parameter
K_1	Chemical reaction parameter
f'	Velocity (dimensionless)
η	Variable
θ	Temperature distribution (dimensionless)
ϕ	Concentration distribution (dimensionless)

References

1. Choi, U.S.; Eastman, J.A. Enhancing thermal conductivity of fluids with nanoparticles. In Proceedings of the ASME International Mechanical Engineering Congress and Exposition (IMECE), San Francisco, CA, USA, 12–17 November 1995.
2. Aslfattahi, N.; Samylingam, L.; Abdelrazik, A.S.; Arifutzzaman, A.; Saidur, R. MXene based new class of silicone oil nanofluids for the performance improvement of concentrated photovoltaic thermal collector. *Sol. Energy Mater. Sol. Cells* **2020**, *211*, 110526. [CrossRef]
3. Abbas, F.; Ali, H.M.; Shah, T.R.; Babar, H.; Janjua, M.M.; Sajjad, U.; Amer, M. Nanofluid: Potential evaluation in automotive radiator. *J. Mol. Liq.* **2020**, *297*, 112014. [CrossRef]
4. Bakthavatchalam, B.; Habib, K.; Saidur, R.; Saha, B.B.; Irshad, K. Comprehensive study on nanofluid and ionanofluid for heat transfer enhancement: A review on current and future perspective. *J. Mol. Liq.* **2020**, *305*, 112787. [CrossRef]
5. Ghahremanian, S.; Abbassi, A.; Mansoori, Z.; Toghraie, D. Investigation the nanofluid flow through a nanochannel to study the effect of nanoparticles on the condensation phenomena. *J. Mol. Liq.* **2020**, *311*, 113310. [CrossRef]
6. Cacua, K.; Buitrago-Sierra, R.; Pabon, E.; Gallego, A.; Zapata, C. Bernardo HerreraNanofluids stability effect on a thermosyphon thermal performance. *Int. J. Therm. Sci.* **2020**, *153*, 106347. [CrossRef]
7. Lund, L.A.; Omar, Z.; Khan, I.; Sherif, E.-S.M.; Abdo, H.S. Stability Analysis of the Magnetized Casson Nanofluid Propagating through an Exponentially Shrinking/Stretching Plate: Dual Solutions. *Symmetry* **2020**, *12*, 1162. [CrossRef]

8. Rasool, G.; Chamkha, A.J.; Muhammad, T.; Shafiq, A.; Khan, I. Darcy-Forchheimer relation in Casson type MHD nanofluid flow over non-linear stretching surface. *Prop. Power Res.* **2020**, *9*, 159–168. [CrossRef]

9. Wakif, A.; Boulahia, Z.; Sehaqui, R. Numerical analysis of the onset of longitudinal convective rolls in a porous medium saturated by an electrically conducting nanofluid in the presence of an external magnetic field. *Res. Phys.* **2017**, *7*, 2134–2152. [CrossRef]

10. Hayat, T.; Aziz, A.; Muhammad, T.; Alsaedi, A. Active and passive controls of 3D nanofluid flow by a convectively heated nonlinear stretching surface. *Phy. Scr.* **2019**, *94*, 085704. [CrossRef]

11. Rasool, G.; Wakif, A. Numerical spectral examination of EMHD mixed convective flow of second-grade nanofluid towards a vertical Riga plate using an advanced version of the revised Buongiorno's nanofluid model. *J. Therm. Anal. Calorim.* **2020**, accepted. [CrossRef]

12. Chamkha, A.J. Coupled heat and mass transfer by natural convection about a truncated cone in the presence of magnetic field and radiation effects. *Numer. Heat Trans. Part A* **2001**, *39*, 511–530. [CrossRef]

13. Mohebbi, R.; Izadi, M.; Chamkha, A.J. Heat source location and natural convection in a c-shaped enclosure saturated by a nanofluid. *Phys. Fluids* **2017**, *29*, 122009. [CrossRef]

14. Rasool, G.; Shafiq, A.; Khan, I.; Baleanu, D.; Nisar, K.S.; Shahzadi, G. Entropy generation and consequences of MHD in Darcy–Forchheimer nanofluid flow bounded by non-linearly stretching surface. *Symmetry* **2020**, *12*, 652. [CrossRef]

15. Lund, L.A.; Omar, Z.; Raza, J.; Khan, I.; Sherif, E.-S.M. Effects of Stefan Blowing and Slip Conditions on Unsteady MHD Casson Nanofluid Flow Over an Unsteady Shrinking Sheet: Dual Solutions. *Symmetry* **2020**, *12*, 487. [CrossRef]

16. Sohail, M.; Naz, R.; Abdelsalam, S.I. On the onset of entropy generation for a nanofluid with thermal radiation and gyrotactic microorganisms through 3D flows. *Phys. Scr.* **2020**, *95*, 045206. [CrossRef]

17. Rasool, G.; Zhang, T.; Chamkha, A.J.; Shafiq, A.; Tlili, I.; Shahzadi, G. Entropy generation and consequences of binary chemical reaction on MHD Darcy–Forchheimer Williamson nanofluid flow over non-linearly stretching surface. *Entropy* **2020**, *22*, 18. [CrossRef]

18. Hayat, T.; Aziz, A.; Muhammad, T.; Alsaedi, A. An optimal analysis for Darcy–Forchheimer 3D flow of nanofluid with convective condition and homogeneous–heterogeneous reactions. *Phys. Lett. A* **2018**, *382*, 2846–2855. [CrossRef]

19. Rasool, G.; Shafiq, A.; Durur, H. Darcy-Forchheimer relation in Magnetohydrodynamic Jeffrey nanofluid flow over stretching surface. *Discret. Contin. Dyn. Syst.-S* **2020**, *30*, 1632–1937.

20. Wakif, A.; Boulahia, Z.; Sehaqui, R. A semi-analytical analysis of electro-thermo-hydrodynamic stability in dielectric nanofluids using Buongiorno's mathematical model together with more realistic boundary conditions. *Res. Phys.* **2018**, *9*, 1438–1454. [CrossRef]

21. Reddy, S.; Chamkha, A.J. Soret and Dufour effects on MHD convective flow of Al_2O_3-Water and TiO_2-Water Nanofluids Past a Stretching Sheet in Porous Media with Heat Generation/Absorption. *Adv. Powder Technol.* **2016**, *27*, 1207–1218. [CrossRef]

22. Rasool, G.; Zhang, T.; Shafiq, A. Second grade nanofluidic flow past a convectively heated vertical Riga plate. *Phys. Scr.* **2019**, *94*, 125212. [CrossRef]

23. Wakif, A.; Boulahia, Z.; Ali, F.; Eid, M.R.; Sehaqui, R. Numerical Analysis of the Unsteady Natural Convection MHD Couette Nanofluid Flow in the Presence of Thermal Radiation Using Single and Two-Phase Nanofluid Models for Cu–Water Nanofluids. *Int. J. Appl. Comput. Math.* **2018**, *4*, 81. [CrossRef]

24. Ghalambaz, M.; Chamkha, A.J.; Wen, D. Natural convective flow and heat transfer of nano-encapsulated phase change materials (NEPCMs) in a cavity. *Int. J. Heat Mass Trans.* **2019**, *138*, 738–749. [CrossRef]

25. Rasool, G.; Zhang, T. Darcy-Forchheimer nanofluidic flow manifested with Cattaneo-Christov theory of heat and mass flux over non-linearly stretching surface. *PLoS ONE* **2019**, *14*, e0221302. [CrossRef] [PubMed]

26. Hayat, T.; Khan, M.I.; Khan, T.A.; Khan, M.I.; Ahmad, S.; Alsaedi, A. Entropy generation in Darcy-Forchheimer bidirectional flow of water-based carbon nanotubes with convective boundary conditions. *J. Mol. Liq.* **2018**, *265*, 629–638. [CrossRef]

27. Rasool, G.; Shafiq, A.; Khalique, C.M.; Zhang, T. Magnetohydrodynamic Darcy–Forchheimer nanofluid flow over a nonlinear stretching sheet. *Phys. Scr.* **2019**, *94*, 105251. [CrossRef]

28. Lund, L.A.; Omar, Z.; Raza, J.; Khan, I. Magnetohydrodynamic flow of Cu–Fe_3O_4/H_2O hybrid nanofluid with effect of viscous dissipation: dual similarity solutions. *J. Therm. Anal. Calorim* **2020**. [CrossRef]

29. Sohail, M.; Naz, R. Modified heat and mass transmission models in the magnetohydrodynamic flow of Sutterby nanofluid in stretching cylinder. *Phys. A Stat. Mech. Its Appl.* **2020**, *549*, 124088. [CrossRef]

30. Darcy, H. *Les Fontaines Publiques de la Ville de Dijon*; Victor Dalmont: Paris, France, 1856.

31. Forchheimer, P. Wasserbewegung durch boden. *Z. Ver. Deutsch. Ing.* **1901**, *45*, 1782–1788.

32. Muskat, M. *The Flow of Homogeneous Fluids Through Porous Media*; Edwards: Ann Arbor, MI, USA, 1946.

33. Muhammad, T.; Rafique, K.; Asma, M.; Alghamdi, M. Darcy–Forchheimer flow over an exponentially stretching curved surface with Cattaneo–Christov double diffusion. *Physica A* **2020**, accepted. [CrossRef]

34. Ambreen, T.; Saleem, A.; Park, C.W. Analysis of hydro-thermal and entropy generation characteristics of nanofluid in an aluminium foam heat sink by employing Darcy-Forchheimer-Brinkman model coupled with multiphase Eulerian model. *App. Therm. Eng.* **2020**, *173*, 115231. [CrossRef]

35. Ullah, M.Z.; Alshomrani, A.S.; Alghamdi, M. Significance of Arrhenius activation energy in Darcy–Forchheimer 3D rotating flow of nanofluid with radiative heat transfer. *Phys. A Stat. Mech. Its Appl.* **2020**, *550*, 124024. [CrossRef]

36. Huda, N.U.; Hamid, A.; Khan, M. Impact of Cattaneo-Christov model on Darcy–Forchheimer flow of ethylene glycol basefluid over a moving needle. *J. Mater. Res. Technol.* **2020**, accepted.

37. Sajid, T.; Sagheer, M.; Hussain, S.; Bilal, M. Darcy-Forchheimer flow of Maxwell nanofluid flow with nonlinear thermal radiation and activation energy. *AIP Adv.* **2018**, *8*, 035102. [CrossRef]

38. Jiang, N.; Studer, E.; Podvin, B. Physical modeling of simultaneous heat and mass transfer: Species interdiffusion, Soret effect and Dufour effect. *Int. J. Heat Mass Trans.* **2020**, *15*, 119758. [CrossRef]

39. Liu, Q.; Feng, X.-B.; Xu, X.-T.; He, Y.-L. Multiple-relaxation-time lattice Boltzmann model for double-diffusive convection with Dufour and Soret effects. *Int. J. Heat Mass Trans.* **2019**, *13*, 713–719. [CrossRef]

40. Sardar, H.; Ahmad, L.; Khan, M.; Alshomrani, A.S. Investigation of mixed convection flow of Carreau nanofluid over a wedge in the presence of Soret and Dufour effects. *Int. J. Heat Mass Trans.* **2019**, *137*, 809–822. [CrossRef]

41. Hamid, A.; Khan, M. Impacts of binary chemical reaction with activation energy on unsteady flow of magneto-Williamson nanofluid. *J. Mol. Liq.* **2018**, *262*, 435–442. [CrossRef]

42. Dhlamini, M.; Kameswaran, P.K.; Sibanda, P.; Motsa, S.; Mondal, H. Activation energy and binary chemical reaction effects in mixed convective nanofluid flow with convective boundary conditions. *J. Comput. Des. Eng.* **2019**, *6*, 149–158. [CrossRef]

43. Khan, U.; Zaib, A.; Khan, I.; Nisar, K.S. Activation energy on MHD flow of titanium alloy (Ti$_6$Al$_4$V) nanoparticle along with a cross flow and stream wise direction with binary chemical reaction and non-linear radiation: Dual Solutions. *J. Mater. Res. Technol.* **2020**, *9*, 188–199. [CrossRef]

44. Pal, D.; Mondal, H. Effects of Soret Dufour, chemical reaction and thermal radiation on MHD non-Darcy unsteady mixed convective heat and mass transfer over a stretching sheet. *Commun. Nonlinear Sci. Numer. Simul.* **2011**, *16*, 1942–1958. [CrossRef]

45. Turkyilmazoglu, M. Three dimensional MHD flow and heat transfer over a stretching/shrinking surface in a viscoelastic fluid with various physical effects. *Int. J. Heat Mass Trans.* **2014**, *78*, 150–155. [CrossRef]